Neuron, Vol. 38, 237–252, April 24, 2003, Copyright ©2003 by Cell Press

Unitary Assembly of Presynaptic Active Zones from Piccolo-Bassoon Transport Vesicles

Mika Shapira,[1,5] R. Grace Zhai,[2,5,6] Thomas Dresbach,[3] Tal Bresler,[1] Viviana I. Torres,[4] Eckart D. Gundelfinger,[3] Noam E. Ziv,[1,*] and Craig C. Garner[2,4,*]

[1]Rappaport Institute and
Department of Anatomy and Cell Biology
Technion Faculty of Medicine
Haifa
Israel

[2]Department of Neurobiology
University of Alabama at Birmingham
Birmingham, Alabama 35294

[3]Department of Neurochemistry and
Molecular Biology
Leibniz Institute for Neurobiology
D-39118 Magdeburg
Germany

[4]Department of Psychiatry and Behavioral Science
Nancy Pritzker Laboratory
Stanford University
Palo Alto, California 94304

Summary

Recent studies indicate that active zones (AZs)—sites of neurotransmitter release—may be assembled from preassembled AZ precursor vesicles inserted into the presynaptic plasma membrane. Here we report that one putative AZ precursor vesicle of CNS synapses—the Piccolo-Bassoon transport vesicle (PTV)—carries a comprehensive set of AZ proteins genetically and functionally coupled to synaptic vesicle exocytosis. Time-lapse imaging reveals that PTVs are highly mobile, consistent with a role in intracellular transport. Quantitative analysis reveals that the Bassoon, Piccolo, and RIM content of individual PTVs is, on average, half of that of individual presynaptic boutons and shows that the synaptic content of these molecules can be quantitatively accounted for by incorporation of integer numbers (typically two to three) of PTVs into presynaptic membranes. These findings suggest that AZs are assembled from unitary amounts of AZ material carried on PTVs.

Introduction

The active zone (AZ) is a highly specialized region of the presynaptic plasma membrane where synaptic vesicles (SVs) dock, fuse, and release their neurotransmitters into the synaptic cleft. This region is characterized ultrastructurally as an electron dense meshwork of cytoskeletal filaments that are intimately associated with the plasma membrane, embedded with clusters of SVs, and juxtaposed to the electron dense postsynaptic density (PSD). The electron dense cytoskeletal matrix associated with the active zone (CAZ) is thought to play a fundamental role in defining neurotransmitter release sites, keeping the active zone in register with the postsynaptic reception apparatus, and regulating the mobilization of SVs and the refilling of release sites (reviewed in Dresbach et al., 2001).

Molecular analysis has revealed that several multimeric protein complexes are found at the mature presynaptic terminal (Brose et al., 2000; Sudhof, 2000; Dresbach et al., 2001). One of these includes components of the SNARE complex including Syntaxin, SynaptobrevinII/VAMP2, and SNAP25 that promote docking and/or fusion of SVs with the active zonal plasma membrane (Sudhof, 2000). Another includes Munc18, Munc13, Synaptotagmin, and Complexin2, molecules shown to interact with components of the SNARE complex and to regulate SV exocytosis (Brose et al., 2000). Finally, a collection of presynaptic modular proteins, which includes Piccolo, Bassoon, RIMs, CASK, CAST, Velis, and Mints, is thought to perform scaffolding functions at AZs, that is, to spatially organize elements of the AZ, including voltage-gated calcium channels and the SV endo- and exocytotic machinery (Dresbach et al., 2001; Ohtsuka et al., 2002; Schoch et al., 2002).

In spite of enormous progress made toward the elucidation of AZ structure and function, the cellular and molecular mechanisms that underlie the formation of AZs during synaptogenesis as well as the mechanisms that underlie the recruitment of presynaptic molecules to nascent AZs are not well understood. Time-lapse imaging studies have shown that individual synaptic connections can form relatively quickly (reviewed in Ziv and Garner, 2001; Garner et al., 2002). In particular, the formation of functional AZs capable of recycling SVs has been observed to occur in vitro within 30–60 min of initial axo-dendritic contact (Ahmari et al., 2000; Vardinon-Friedman et al., 2000; Colicos et al., 2001; see also Okabe et al., 2001; Bresler et al., 2001; Antonova et al., 2001). These observations have led to the suggestion that presynaptic compartments may be assembled from macromolecular complexes transported along axons and recruited to nascent presynaptic membranes as preformed precursors (Ahmari et al., 2000; Zhai et al., 2001; see also Roos and Kelly, 2000).

In a previous study, we found that the CAZ proteins Piccolo and Bassoon are carried along axons on a novel class of dense-core vesicles, referred to as Piccolo-Bassoon transport vesicles (PTVs) (Zhai et al., 2001). Intriguingly, additional AZ molecules, including Syntaxin, SNAP25, and N-cadherin, were found on this vesicle. As both Piccolo and Bassoon clusters were found at nascent synapses as soon as these displayed a capacity for activity-dependent recycling of SVs (Vardinon-Friedman et al., 2000; Zhai et al., 2001), we suggested that PTVs may be AZ precursor vesicles.

PTVs have predicted surface areas ($\sim$0.020 μm^2) comparable to those of AZs in the rat hippocampus (mean =

*Correspondence: garner@stanford.edu (C.C.G.), noamz@netvision.net.il (N.E.Z.)

[5]These authors contributed equally to this work.

[6]Present address: Department of Molecular Human Genetics, Baylor College of Medicine, Houston, Texas 77030.

0.039 μm^2; Schikorski and Stevens, 1997) and are very uniform in size (80.2 $\pm$ 8.1; Zhai et al., 2001). This raises an intriguing possibility that new functional AZs may be assembled from just a very small number of PTVs that carry unitary amounts of AZ material. It is even imaginable that the fusion of one such precursor vesicle with the nascent presynaptic membrane may be sufficient for the formation of a new functional AZ, raising the possibility that AZ formation is an "all or none" process.

While this mechanism is appealing in its apparent simplicity, it introduces fundamental issues that have yet to be addressed. First, for a single precursor vesicle to be sufficient for the formation of a new functional AZ, it would have to carry a full set of the molecules essential for transforming a patch of presynaptic membrane into a functional active zone. Otherwise, nonfunctional AZs could be formed due to the absence of an essential molecule such as Munc-13-1 or Munc-18-1 (Augustin et al., 1999; Verhage et al., 2000). Second, the amounts of each protein carried on each PTV would have to be quantitatively similar to the amounts typically found at presynaptic AZs.

Alternatively, AZs could be assembled from multiple precursor vesicles that vary in their molecular content. For example, PTVs may be formed via multiple pathways, resulting in distinct populations of vesicles carrying different subsets of AZ molecules. Variability in PTV content could also result from a single, low-fidelity biogenesis pathway. Either way, the stringent requirements placed on the contents of individual vesicles would be relaxed. As a consequence, however, AZ assembly would become more complicated and less efficient. Thus, important questions remain unanswered: Do PTVs carry a comprehensive set of essential AZ molecules? Do all PTVs carry the same set of AZ molecules? How many PTVs are required to deliver the amounts of AZ molecules found at presynaptic boutons? Are AZs assembled in unitary fashion from AZ material carried on PTVs?

Here we report that in addition to Piccolo and Bassoon, PTVs carry a comprehensive set of proteins genetically and functionally coupled to SV exocytosis. Immunohistochemical analysis confirmed that these molecules are carried on PTVs, although some heterogeneity in the molecular contents of individual PTVs was observed. Live imaging of neurons expressing GFP-tagged Bassoon revealed that axons contain numerous nonsynaptic, highly mobile Bassoon puncta with mobility characteristics typical of transport vesicles. Quantitative immunofluorescence analysis of such nonsynaptic puncta suggests that individual PTVs carry, on average, about half of the Bassoon, Piccolo, and RIM content of individual synapses. Furthermore, this analysis suggests that integer numbers of PTVs (typically two to three) are incorporated into presynaptic membranes to make up the entire synaptic content of Bassoon, Piccolo, and RIM. Finally, our analysis indicates that some heterogeneity in PTV composition makes complete AZ formation dependent on the fusion of more than one PTV. Together, these findings suggest that AZs are assembled from unitary amounts of AZ proteins carried on two to three PTVs.

Results

PTVs Carry a Comprehensive Set of Essential AZ Molecules

In a previous study (Zhai et al., 2001), we have found that the CAZ proteins Piccolo and Bassoon are carried on the cytoplasmic aspect of 80 nm dense-core vesicles, thereafter named "PTVs." Furthermore, immunoisolated PTVs were found to contain additional AZ proteins, such as Syntaxin1a and SNAP-25, but not SV proteins or periactive zonal proteins. These findings suggested that PTVs might constitute a novel form of AZ precursor vesicles whose fusion with the plasma membrane at nascent presynaptic sites may lead to deposition of proteins involved in SV exocytosis and ultimately to the formation of new AZs (Zhai et al., 2001).

To further test this hypothesis, we examined whether proteins known to *regulate* SV exocytosis were also associated with PTVs. These included the Syntaxin binding protein Munc18, the phorbol ester binding protein Munc13, the GTPase Rab3a/c, and the Rab3a/c effecter protein RIM (Ishizuka et al., 1995; Takahashi et al., 1995; Augustin et al., 1999; Verhage et al., 2000; Schoch et al., 2002). All four molecules were detected on PTVs immunoisolated with Piccolo antibodies but not on material immunoisolated with an irrelevant IgG (Figure 1). We also examined whether the core (α1) and auxiliary (β1) subunits of the N-type calcium channel were present on PTVs. Both were found to be selectively enriched in Piccolo immunoisolated material (Figure 1). As controls for these experiments, we examined if the SV proteins Synaptophysin and VAMP2/SynaptobrevinII were present in this material, but neither were found (Figure 1; see also Zhai et al., 2001), confirming that this material does not contain discernable amounts of SVs. In addition, we examined whether proteins of the postsynaptic compartment, such as NR1, a subunit of the NMDA receptor, were contaminating our PTV preparation. Although NR1 is expressed at this time of development and is seen to float into the 0.8/1.2 M interface of the discontinuous sucrose gradients (Figure 1B), very little NR1 was seen in the 0.3/0.8 M sucrose interface used to isolate PTVs (Figure 1B) and was not coimmunoisolated with Piccolo antibodies from the 0.3/0.8 M sucrose fractions used in our studies. These data support our conclusion that these PTV preparations are not contaminated with nascent synaptic junctions.

The presence of these AZ molecules on PTVs was confirmed by double-label immunofluorescence microscopy as performed previously (Zhai et al., 2001). Specifically, axonal growth cones from hippocampal neurons 4 days in vitro (DIV) were labeled with antibodies against Piccolo and each of the aforementioned AZ proteins. Colocalization of Piccolo immunopositive puncta with RIM, Rab3A, and Munc18 immunopositive puncta was readily observed (Figure 2). However, for the others, including Munc13 and the calcium channel subunits, this latter confirmatory analysis was not possible either because the antibodies currently available were not suitable for immunofluorescence microscopy or because, like Syntaxin and SNAP-25, they are not restricted to discrete structures in immature neurons (data not shown).

Given the limited spatial resolution of fluorescent mi-

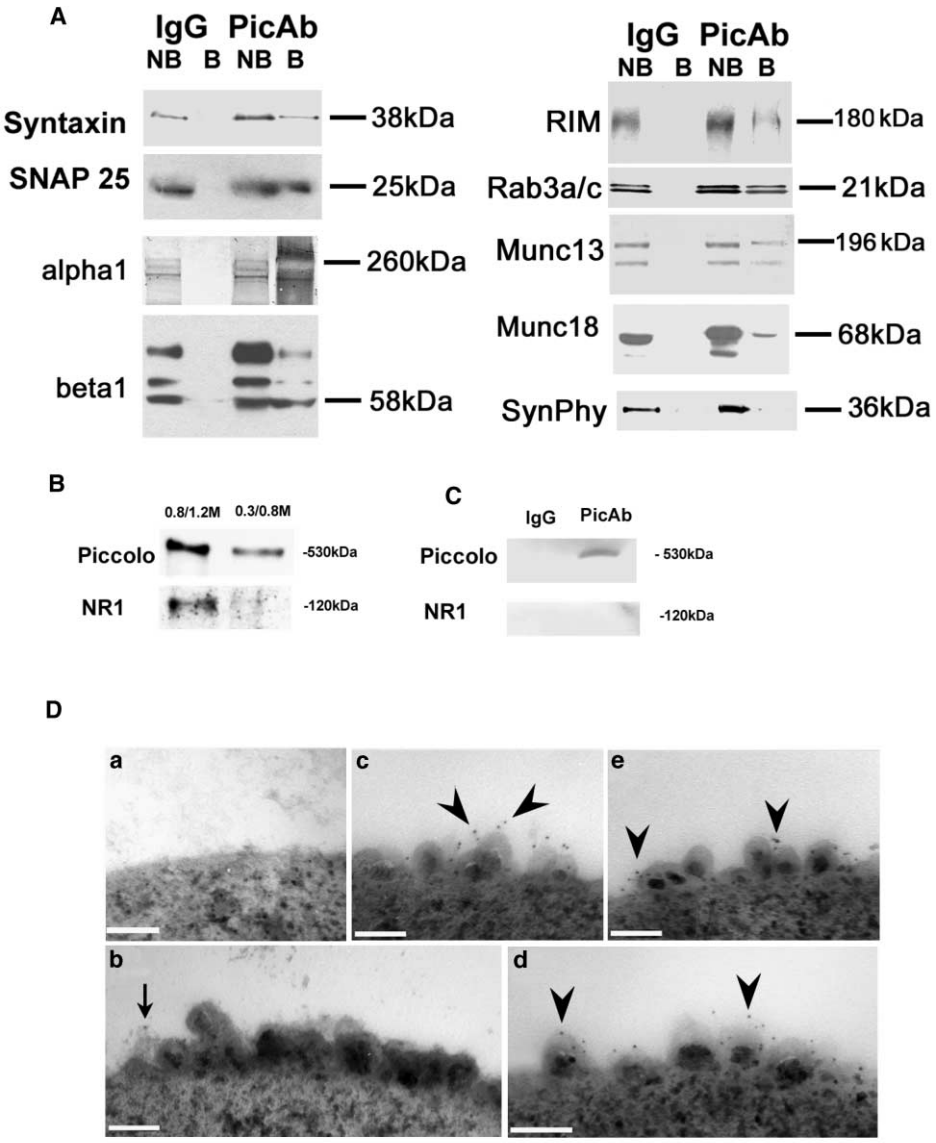

Figure 1. PTVs Contain Components of the Exocytosis Machinery

(A) Light membrane fractions (0.3/0.8 M sucrose) were incubated with Piccolo-rAb beads or irrelevant IgG beads. The beads were then collected and washed extensively. The supernatant fractions were saved as the nonbound subfraction (NB). The bead-bound subfraction (B) and NB fractions were resolved by SDS-PAGE and subjected to Western blotting to detect the presence of Syntaxin, SNAP 25, α1, and β1 subunits of the N-type calcium channel, Munc18, RIM, Rab3a/c, Munc13, and Synaptophysin (SynPhy).

(B) Western blots of membrane fractions taken from a flotation gradient and probed with antibodies against Piccolo and the NR1 subunit of the NMDA receptor. While both synaptic proteins are found in the 0.8/1.2 M sucrose interface, very little NR1 is found in the 0.3/0.8 M sucrose interface used to immunoisolate PTVs.

(C) Western blots of PTVs immunoisolated with Piccolo antibodies or control IgGs and probed with antibodies to Piccolo and NR1. Piccolo is immunoisolated but not NR1. These data indicate that PTVs contain AZ components but not SV proteins or components of the postsynapse.

(D) Immuno-EM confirms that specific AZ proteins are directly associated with 80 nm electron dense vesicles immunoisolated using anti-Piccolo antibodies. EM of control IgG beads (Da) or Piccolo-rAb beads (Db–De) incubated with light membrane fractions. After extensive wash, beads were incubated with synaptophysin mAb (Db), Bassoon mAb (Dc), RIM mAb (Dd), or Munc18 mAb (De), washed, and then incubated with anti-mouse secondary antibodies conjugated to 5 nm gold particles. The beads were then collected and washed extensively, fixed, and processed for EM. PTVs isolated by Piccolo-rAb beads could be labeled by Bassoon, RIM, or Munc18 antibodies (arrowheads in [Dc], [Dd], and [De], respectively) but not Synaptophysin antibodies (Db). Note that there is a gold particle present in the view (arrow in panel Db); however, it is not decorating PTVs.

Scale bars, 100 nm in all panels.

croscopy, we sought to confirm the presence of specific AZ proteins on PTVs by electron microscopy (EM). To this end, Piccolo antibodies coupled to magnetic beads were used to immunoisolate PTVs from E18 light membrane fractions. The beads were then treated with either synaptophysin, Bassoon, RIM, or Munc18 antibodies

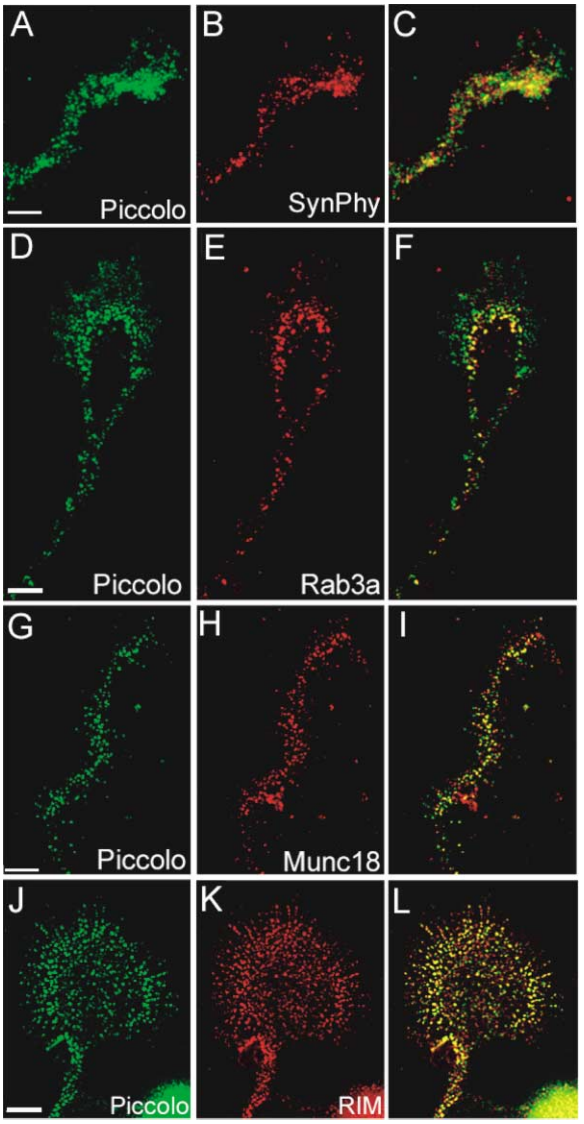

Figure 2. In Growth Cones of Hippocampal Neurons Grown in Low-Density Culture, Piccolo Colocalizes with Components of Active Zones but Not Synaptic Vesicles

Neurons grown in culture for 4 days were double labeled with antibodies against Piccolo (A, D, G, and J) and Synaptophysin (SynPhy) (B), Rab3a (E), Munc18 (H), or RIM (K). Piccolo and Synaptophysin (A–C) exhibited a nonoverlapping punctate pattern (<5% colocalization) similar to that found for Synaptotagmin (see Zhai et al., 2001), indicating that PTVs are distinct from SVs. In contrast, nearly all Piccolo-positive puncta colocalized with Rab3a immunoreactive puncta, while ~50% of the Rab3a puncta were Piccolo positive (D–F), in support of our biochemical data indicating that, in addition to its association with SVs, Rab3a is also present on PTVs. Most Piccolo puncta (~90%) were also positive for Munc18 (G–I) and RIM (J–L), while ~50% of the Munc18 and RIM immunoreactive puncta were Piccolo positive, providing further support for our biochemical data indicating that PTVs carry many proteins involved in SV exocytosis to active zones. Scale bars, 20 μm.

followed by secondary antibodies coupled to 5 nm gold particles. The beads were then fixed and processed for EM. As shown in Figure 1D, beads coated with Piccolo antibodies, unlike beads coated with control IgG, isolate vesicles (~80 nm in diameter) with electron dense centers. Moreover, these vesicles were selectively decorated with antibodies against Bassoon, RIM, and Munc18 but not by antibodies against synaptophysin, confirming that PTVs carry these critical AZ proteins.

In summary, these findings show that PTVs carry a comprehensive set of AZ molecules, providing further support to the hypothesis that the PTV constitutes an important form of an AZ precursor vesicle.

Axons Contain Highly Mobile, Nonsynaptic Bassoon Puncta

Previous studies have shown that packets of SVs in developing axons are highly mobile before being recruited to synaptic sites (Matteoli et al., 1992; Kraszewski et al., 1995; Dai and Peng, 1996; Nakata et al., 1998; Ahmari et al., 2000; Hopf et al., 2002). If PTVs are indeed transport vesicles, they would be expected to display similar mobility characteristics.

In order to study the dynamics of PTVs inside living neurons, we expressed Bassoon tagged with green fluorescent protein (GFP) in cultured hippocampal neurons. To this end, we used a construct in which GFP was fused to amino acid 609 of Bassoon (GFP-Bsn609-3938). This slightly truncated version of Bassoon is recruited effectively to presynapses, and its behavior is practically indistinguishable from that of endogenous Bassoon (T.D. and E.D.G., unpublished data and see below). Hippocampal neuronal cultures were transfected with GFP-Bsn609-3938 at 6 DIV and observed at days 8–11, the period at which peak rates of synaptogenesis occur in our preparations. GFP-Bsn609-3938 displayed an expression pattern consisting of fluorescent puncta of various sizes scattered along long and thin processes, presumably axons. To verify that GFP-Bsn609-3938 was not highly overexpressed, Bsn609-3938-expressing neurons were fixed and immunolabeled against Bassoon. Quantitative analysis revealed that the fluorescence intensities of Bassoon puncta in neurons expressing GFP-Bsn609-3938 were only 22% on average higher than those in neurons not expressing the exogenous molecule, suggesting that Bassoon overexpression levels were relatively modest.

Time-lapse confocal microscopy of GFP-Bsn609-3938 puncta immediately revealed that many of the smaller puncta were highly mobile. In fact, we could not collect image stacks or improve image quality by frame averaging because many puncta changed position too rapidly. Thus, only single sections at slow scan rates (required to improve the signal/noise ratio) were collected, limiting sampling rates on our confocal microscope system to ~4 images/min. Images were obtained with the confocal pinhole fully open to maximize the depth of field and minimize effects of focus drift. As static objects in the field remained in perfect focus during these short time-lapse sequences, the mobility of GFP-Bsn609-3938 puncta was not likely to be an artifact of focal drift.

Three populations of GFP-Bsn609-3938 puncta that differed in their mobility characteristics were observed: (1) bright, relatively stationary puncta; (2) very mobile, dimmer puncta (maximal velocities > 0.35 μm/s); and (3) puncta that displayed moderate rates of movement (maximal velocities ~0.1 μm/s). Similar to nonsynaptic

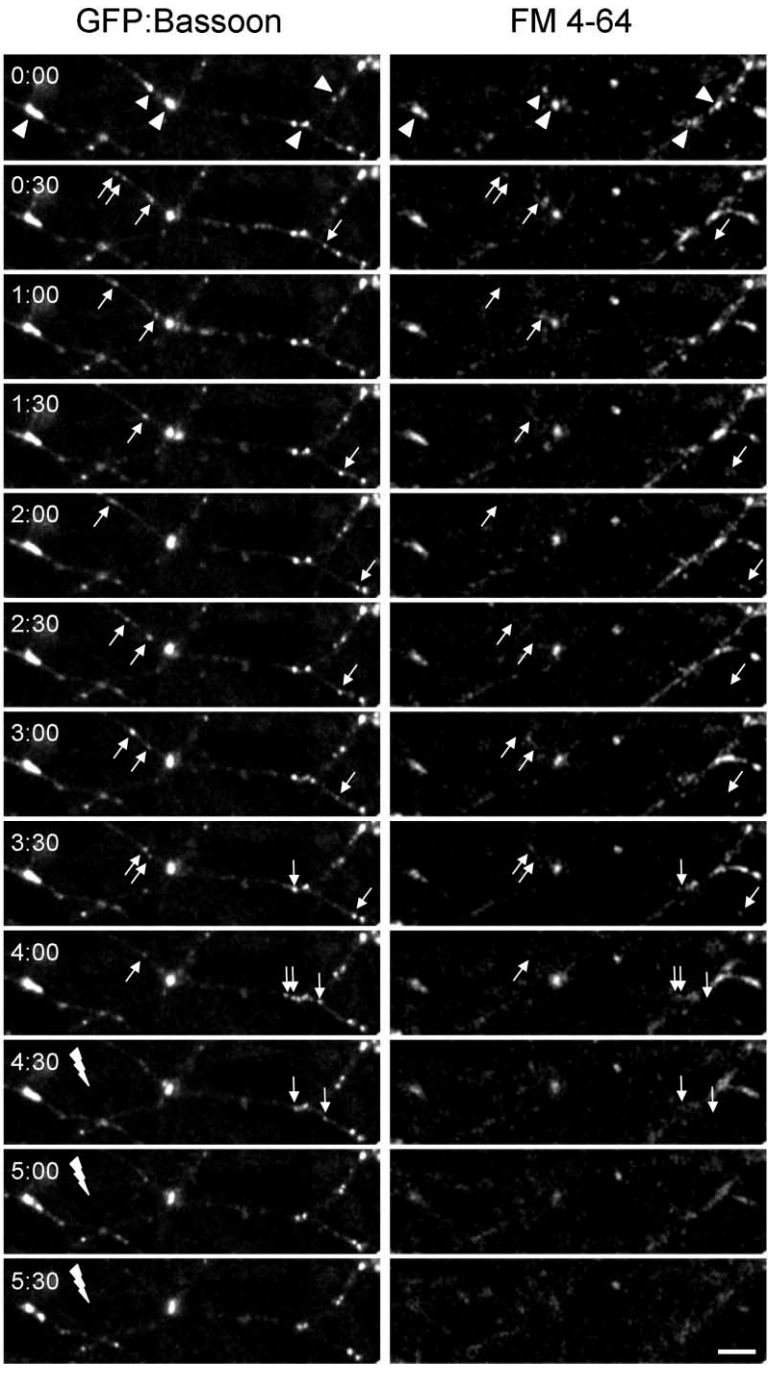

Figure 3. Time Lapse of GFP-Bsn609-3938 Puncta and FM 4-64-Labeled Functional Boutons

Many of the GFP-Bsn609-3938 puncta (left column) are highly mobile (arrows) and not associated with FM 4-64-labeled functional presynaptic boutons (right column), while many of the larger puncta are stationary and associated with FM 4-64-labeled presynaptic boutons (arrowheads, t = 0). Field stimulation delivered at 10 Hz from 4:30 onward (lightning bolts) led to the release of FM 4-64, confirming the presynaptic identity of the FM 4-64-labeled puncta. Note the GFP-Bsn609-3938 cluster marked by the small arrowhead at time 0:00. This cluster seemed to fall apart and wander away from its original location. Concomitantly, FM 4-64 labeling at this position was lost. Eight days in vitro. Scale bar, 5 μm.

SV clusters moving along axons (Matteoli et al., 1992; Kraszewski et al., 1995; Dai and Peng, 1996; Ahmari et al., 2000), the mobile GFP-Bsn609-3938 puncta moved in both directions, sometimes stopping, occasionally splitting into smaller puncta or coalescing into less mobile larger clusters.

One time-lapse series is shown in Figure 3. Here many dimmer and smaller GFP-Bsn609-3938 puncta are shown to move along axons in both directions, while the brighter and apparently larger GFP-Bsn609-3938 puncta appear quite stationary. In this experiment, functional presynaptic boutons were colabeled with FM 4-64 to determine whether the stationary Bassoon puncta represented synaptic Bassoon clusters. As shown in Figure 3, most of the larger, brighter, and stationary GFP-Bsn609-3938 puncta colocalized with FM 4-64-labeled puncta. The functional presynaptic identity of these puncta is further supported by the finding that electrical stimulation (120 s at 10 Hz) led to FM 4-64 release from these sites. Conversely, the dimmer, smaller, and mobile puncta did not appear to be associated with FM 4-64-labeled puncta, indicating that these highly dynamic GFP-Bsn609-3938 puncta were nonsynaptic.

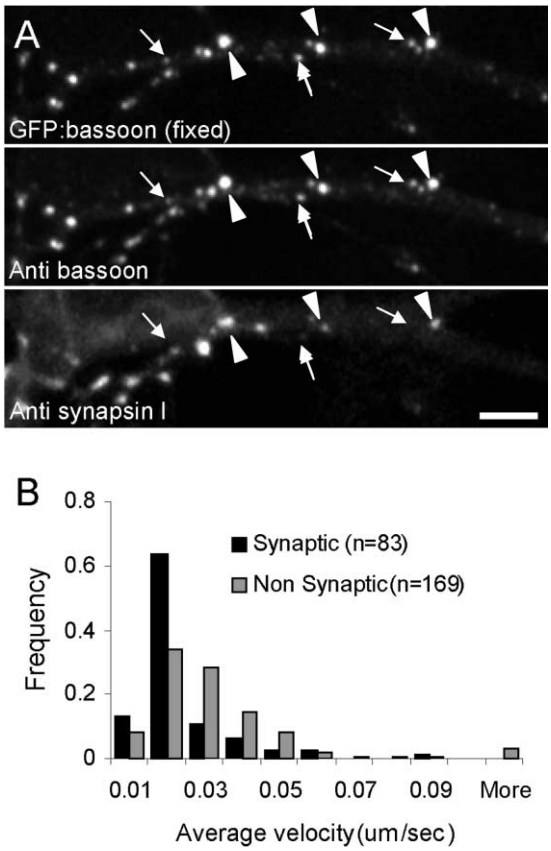

Figure 4. Nonsynaptic GFP-Bsn609-3938 Puncta Are More Mobile than Synaptic GFP-Bsn609-3938 Puncta

(A) An axonal segment of a neuron expressing GFP-Bsn609-3938 after fixation and immunolabeling against Bassoon and Synapsin I. Note that some GFP-Bsn609-3938 clusters colocalized with Synapsin I (arrowheads), while others did not (arrows). Scale bar, 5 μm.

(B) Comparison of average motilities displayed by synaptic and nonsynaptic GFP-Bsn609-3938 clusters. Note that for nonsynaptic puncta these values are gross underestimates, as the most mobile Synapsin I-negative GFP-Bsn609-3938 clusters eluded analysis (see text for details).

These conclusions are supported by a set of time-lapse recordings of GFP-Bsn609-3938 in which the preparations were immunolabeled with Synapsin I, a ubiquitous presynaptic molecule (De Camilli et al., 1983). Here, neurons expressing GFP-Bsn609-3938 were followed for 3 min at 15 s intervals. The preparations were fixed immediately after the last image was obtained and immunolabeled for Bassoon and Synapsin I (Figure 4A). Then each cluster was categorized as *synaptic* or *nonsynaptic* according to its colocalization with Synapsin I. We then attempted to quantify the velocity of each cluster by analyzing time-lapse images obtained prior to fixation. This proved to be a rather difficult task, as we could not reliably track many of the most mobile clusters at the limited sampling rates used to collect the time-lapse series. Thus, most of the clusters we managed to track were either stationary or clusters that displayed intermittent movements separated by periods of stability. Yet even this imperfect analysis, which clearly underestimated the mobility of many GFP-Bsn609-3938 clusters, revealed that GFP-Bsn609-3938 clusters not associated with Synapsin I were much more mobile than those associated with Synapsin I (Figure 4B). Furthermore, even though we were not able to quantify the mobility of the fastest GFP-Bsn609-3938 clusters, retrospective immunohistochemical analysis clearly showed that these were practically always Synapsin I negative.

In summary, nonsynaptic GFP-Bsn609-3938 puncta display mobility characteristics typical of transport vesicles, strongly indicating that PTVs are bona fide transport particles.

Quantitative Analysis Suggests that Most AZs Are Assembled from Two to Three PTVs

The vesicular nature and uniform size of PTVs indicate that they carry discrete (unitary) amounts of active zonal material. Assuming that AZs are formed by the fusion of PTVs with the presynaptic membrane, how many PTVs are required to deliver the amount of AZ material found at functional presynaptic sites?

To obtain an estimate of this number, we used quantitative immunohistochemistry to compare the Bassoon and Piccolo content of individual PTVs to that of individual presynaptic boutons. To differentiate Bassoon and Piccolo carried on PTVs from synaptic clusters of Bassoon and Piccolo, we performed triple immunolabeling of cultured hippocampal neurons with antibodies against Bassoon (Figures 5A and 5B) or Piccolo (Figure 5E), Synapsin I and ProSAP1, a PSD molecule of glutamatergic synapses (Boeckers et al., 1999). Bassoon or Piccolo clusters that colocalized with both Synapsin I and ProSAP1 were considered to be synaptic, while Bassoon or Piccolo clusters that colocalized with neither were considered to be nonsynaptic and were presumed to represent PTVs. The rationale for this categorization was based on (1) the finding that Synapsin I-negative Bassoon clusters commonly displayed mobility characteristics of transport particles (Figures 3 and 4); and (2) the assumption that the probability of truly nonsynaptic clusters to be positive for both pre- and postsynaptic markers would be very low, as would the probability of truly synaptic clusters to be negative for both synaptic markers (see also Ahmari and Smith, 2002).

The immunofluorescence intensities of Bassoon/Piccolo clusters in 12 fields of view in each culture dish were measured (see Experimental Procedures), and fluorescence intensity histograms were prepared for each population (synaptic and nonsynaptic). This analysis was performed separately for each culture dish ($n > 8$) in order to reduce variability arising from sources such as slight differences in antibody concentrations and fixation conditions. Most experiments were performed at days 8–11 in vitro, as peak rates of synaptogenesis are observed in our preparations during this period, while synaptic density is low enough to perform colocalization analyses with a high level of confidence. Some experiments were performed on less mature preparations, however, to examine age-dependent effects. Figure 5 shows data obtained from three representative preparations at 5, 7, and 9 DIV. Comparing the immunofluorescence intensities of synaptic and nonsynaptic Bassoon and Piccolo populations (presumably proportional to the Bassoon or Piccolo content of each population) sug-

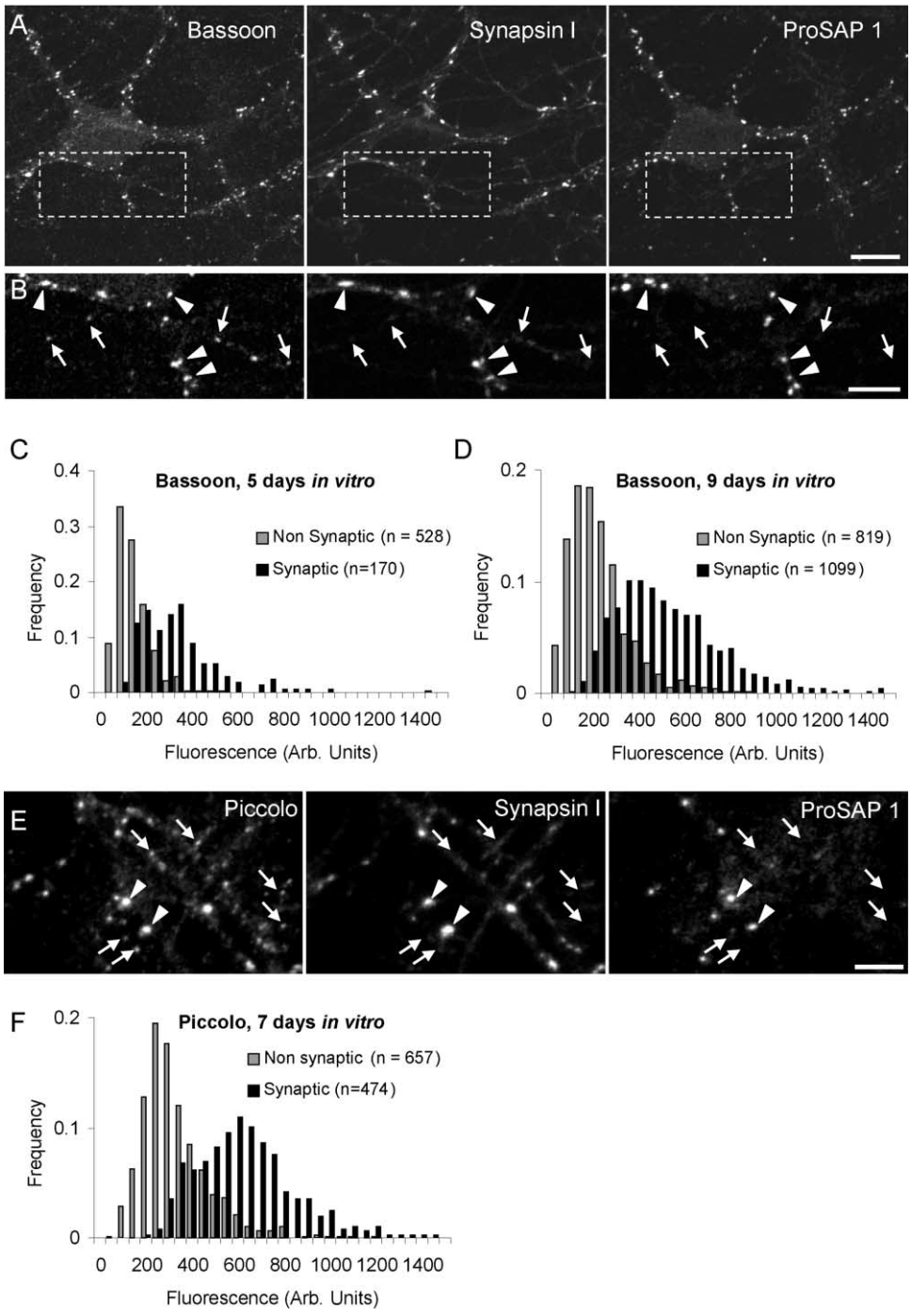

Figure 5. Comparison of Fluorescence Intensities of Synaptic and Nonsynaptic Bassoon and Piccolo Puncta

(A) Neurons grown in culture for 9 DIV, triple labeled for Bassoon, Synapsin I, and ProSAP1.

(B) High magnification of regions enclosed in rectangles in (A). Bassoon clusters that colocalized with both Synapsin I and ProSAP1 (arrowheads) were considered to be synaptic, while those that did not colocalize with either Synapsin I or ProSAP1 (arrows) were referred to as nonsynaptic.

(C) Immunofluorescence intensity histograms of synaptic and nonsynaptic Bassoon, 5 DIV. All data obtained from one culture dish.

(D) Immunofluorescence intensity histograms of synaptic and nonsynaptic Bassoon, 9 DIV. All data obtained from one culture dish.

(E) Neurons cultured 7 DIV were triple labeled for Piccolo, Synapsin I, and ProSAP1. Piccolo clusters that colocalized with both Synapsin I and ProSAP1 (arrowheads) were considered to be synaptic, while those that did not colocalize with either Synapsin I or ProSAP1 (arrows) were referred to as nonsynaptic.

(F) Immunofluorescence intensity histograms of synaptic and nonsynaptic Piccolo clusters.

Scale bars, (A) 10 μm; (B and E) 5 μm.

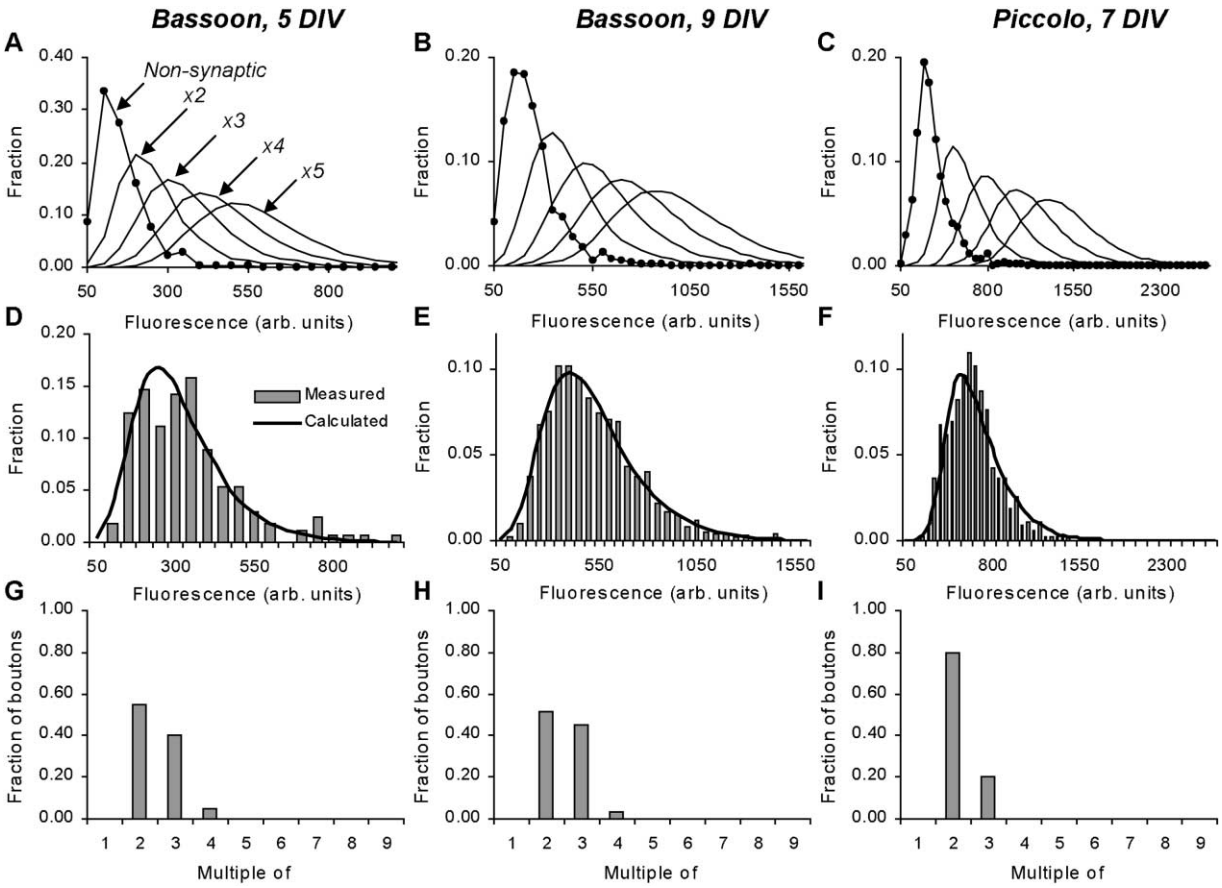

Figure 6. Bassoon and Piccolo Content of Synaptic Clusters Expressed as Multiples of Nonsynaptic Puncta

(A–C) Fluorescence intensity distribution of nonsynaptic Bassoon and Piccolo clusters (filled circles) and calculated fluorescence intensity distributions for integer multiples of nonsynaptic puncta.

(D–F) Weighted sum of curves shown in (A)–(C) fit to experimentally measured fluorescence intensity distributions of synaptic Bassoon and Piccolo clusters. Same data as in Fig 5.

(G–I) Weights used to generate best-fit curves.

gests that, on average, synaptic Bassoon and Piccolo puncta are brighter than nonsynaptic puncta but only by a factor of ~2 (mean synaptic/mean nonsynaptic = 1.972, 1.974, and 1. 967 for data in Figures 5C, 5D, and 5F, respectively).

To further examine the possibility that the Bassoon and Piccolo content of AZs may result from the insertion of integer numbers of unitary amounts of Bassoon and Piccolo carried on PTVs, we performed the following analysis: for each data set, we used the immunofluorescence intensity distribution of the nonsynaptic Bassoon/Piccolo puncta (presumably representing the intensity distribution for single PTVs) to calculate the expected intensity distribution for pairs, triplets, and so on of PTVs (as shown in Figures 6A–6C for the data of Figure 5). Then we attempted to fit these curves to the immunofluorescence intensity distribution of the synaptic population. As shown in Figures 6D–6I, the best match was obtained when we assumed that the Bassoon and Piccolo content of most synapses was a multiple of two unitary amounts of nonsynaptic Bassoon and Piccolo, while the rest contained multiples of three and four unitary amounts (Bassoon, 5 DIV: two, three, and four units—55%, 40%, and 5%, of presynaptic boutons, respectively; Bassoon, 9 DIV: two, three, and four units—52%, 45%, and 3%; Piccolo, 7 DIV: two, three, and four units—80%, 20%, 0%). It should be noted that reasonable fits could be obtained with slightly different values, but these did not alter the general outcome of this analysis.

Additional evidence for unitary relationships between amounts of AZ material carried by PTVs and that found at synapses was obtained by performing a similar analysis for the fluorescent intensities of synaptic and nonsynaptic GFP-Bsn609-3938. Neurons expressing GFP-Bsn609-3938 were fixed immediately after time-lapse imaging and subsequently immunolabeled for Bassoon and Synapsin I (Figure 4A). The fluorescence intensity of each GFP-Bsn609-3938 cluster was measured, and each cluster was categorized as synaptic or nonsynaptic according to its colocalization with Synapsin I. As noted above, synaptic clusters of GFP-Bsn609-3938 appeared to be brighter than nonsynaptic GFP-Bsn609-3938 puncta (mean synaptic to mean nonsynaptic ratio = 1.914). As the number of GFP-Bsn609-3938 clusters followed in each experiment was rather small (Figure 7A), data from six experiments were pooled together (Figure

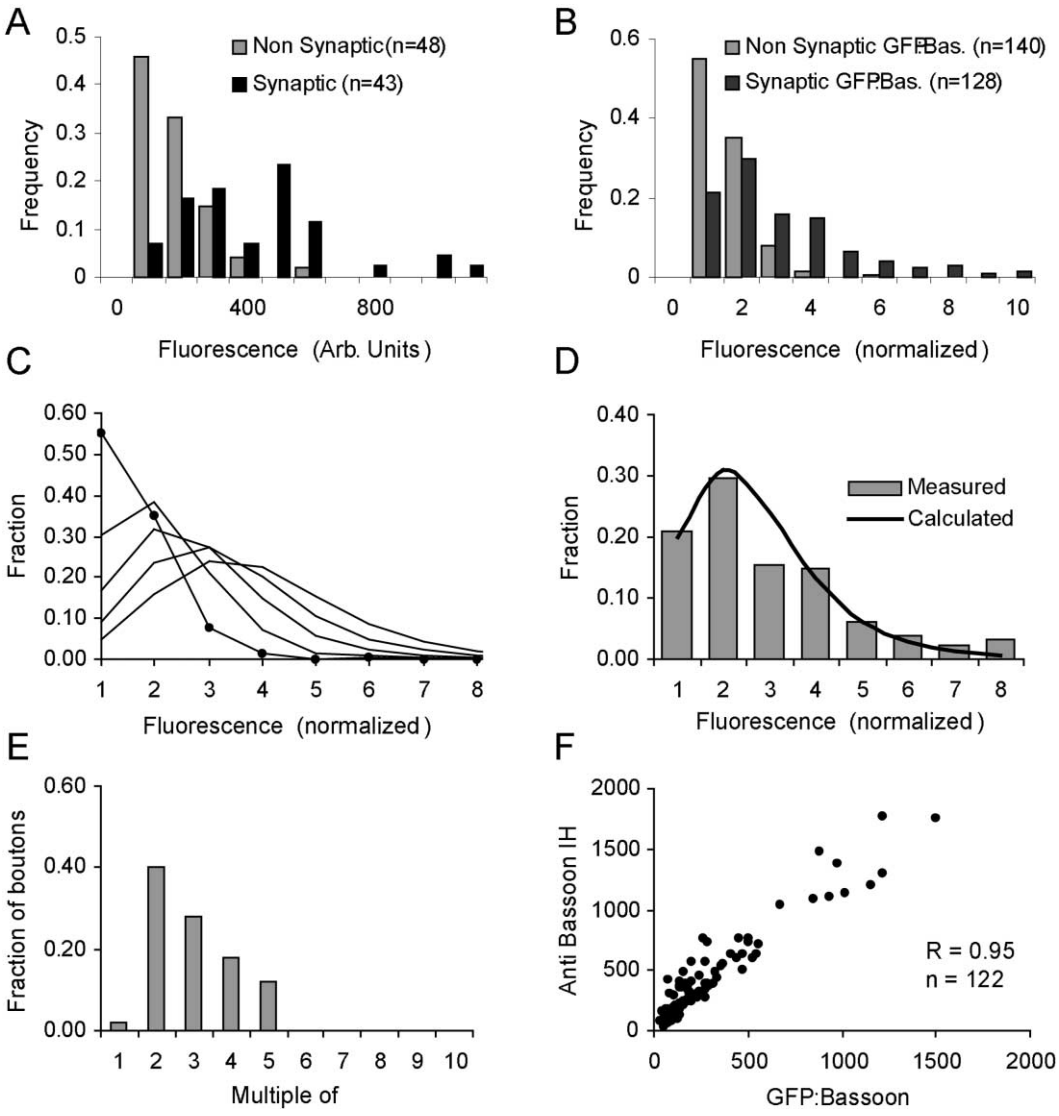

Figure 7. Unitary Relationships of Synaptic and Nonsynaptic GFP-Bsn609-3938

(A) Fluorescence intensity distribution of synaptic and nonsynaptic GFP-Bsn609-3938 clusters. All data shown here was obtained from one GFP-Bsn609-3938-expressing neuron.

(B) Normalized and pooled data for six GFP-Bsn609-3938-expressing neurons. Fluorescence is expressed as multiples of the mean fluorescence of nonsynaptic GFP-Bsn609-3938 clusters in each cell.

(C) Fluorescence intensity distribution of nonsynaptic GFP-Bsn609-3938 (filled circles) and calculated fluorescence intensity distributions for integer multiples of nonsynaptic puncta.

(D) Weighted sum of curves shown in (C) fit to the experimentally measured fluorescence intensity distributions of synaptic GFP-Bsn609-3938 clusters.

(E) Weights used to generate the best-fit curve shown in (D).

(F) Comparison of GFP-Bsn609-3938 fluorescence values of individual puncta to anti-Bassoon immunofluorescence measurements of the same clusters. Data obtained from a single GFP-Bsn609-3938-expressing neuron after fixation and immunolabeling.

7B). Furthermore, because expression levels of GFP-Bsn609-3938 varied from one cell to another, all data were normalized by dividing the fluorescence intensity of each cluster in each cell by the average fluorescence of nonsynaptic GFP-Bsn609-3938 clusters in that cell. Fitting the distribution of synaptic GFP-Bsn609-3938 cluster intensities (Figure 7D) to distribution curves generated on the basis of the intensity distribution of nonsynaptic GFP-Bsn609-3938 clusters (presumably PTVs, Figure 7C) indicated that the content of GFP-Bsn609-3938 in synaptic AZs was primarily a multiple of two to four unitary amounts of GFP-Bsn609-3938 carried on PTVs (Figure 7E, 1, 2, 3, 4, and 5 units—2%, 40%, 28%, 18%, and 12% of presynaptic boutons, respectively). These numbers differ slightly from those obtained by immunofluorescence analysis (Figure 6) but are less accurate due to errors introduced by the normalization process and the small numbers used to generate this fit. Still, they are in general agreement with our hypothesis that AZs are formed in part by the insertion of unitary

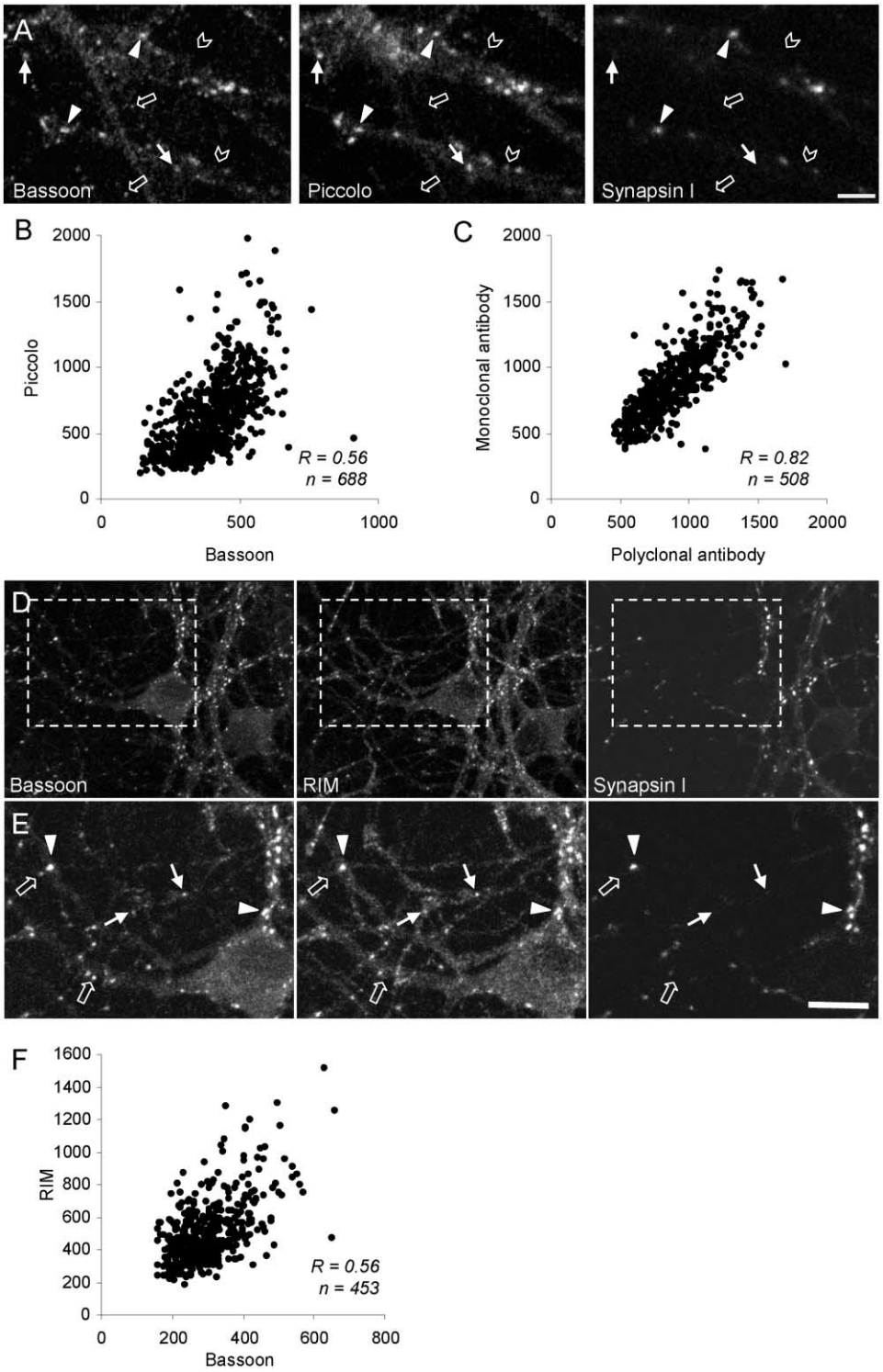

Figure 8. Colocalization of Bassoon, Piccolo, and RIM

(A) Neurons grown in culture for 8 DIV, triple labeled for Bassoon, Piccolo, and Synapsin I. Some Bassoon puncta colocalized with both Piccolo and Synapsin I (arrowheads) and were considered to be synaptic clusters. Most Synapsin I-negative Bassoon clusters colocalized with Piccolo (arrows), although some did not (open arrows). Similarly, some Synapsin I-negative Piccolo puncta did not colocalize with Bassoon (chevrons). Scale bar, 5 μm.

(B) Correlation of Bassoon and Piccolo immunofluorescence at Synapsin I-negative puncta (presumably PTVs).

(C) Correlation of immunofluorescence intensity obtained using two different anti-Bassoon antibodies (a mouse monoclonal and a rabbit polyclonal).

(D) Neurons grown in culture for 8 DIV, triple labeled for Bassoon, RIM, and Synapsin I.

(E) High magnification of regions enclosed in rectangles in (D). RIM clusters that colocalized with both Bassoon and Synapsin I (arrowheads) were considered to be synaptic clusters. RIM clusters that colocalized with Bassoon but not Synapsin I (arrows) were considered to be PTV associated. Note that some Bassoon clusters appeared to be RIM negative (open arrows). Scale bar, 10 μm.

(F) Correlation of RIM and Bassoon immunofluorescence at Bassoon-positive, Synapsin I-negative puncta (presumably PTVs). All data obtained from one culture dish.

amounts of AZ material carried on a small number of PTVs.

Interestingly, a comparison of GFP-Bsn609-3938 and Bassoon immunofluorescence of individual GFP-Bsn609-3938 puncta revealed a linear relationship between these two measures (Figure 7F) with an average correlation coefficient of 0.86 ± 0.07 (n = 6; range 0.74–0.97). This finding implies that Bassoon immunofluorescence is linearly proportional to the amount of Bassoon molecules in immunolabeled structures and indicates that the immunohistochemical methods used in this study provide a quantitative and linear readout of AZ molecule content.

Taken together, these findings suggest that the Bassoon and Piccolo content of presynaptic boutons is typically two to three times greater than that of nonsynaptic Bassoon and Piccolo puncta. These data and the analysis performed above are consistent with the possibility that most new AZs are assembled from two to three PTVs carrying unitary amounts of AZ material.

Individual PTVs Display Some Heterogeneity in Their Molecular Content

The experiments described above seem to suggest that most presynaptic sites are assembled from two to three PTVs, with only a few assembled from single PTVs. One possible explanation for the apparent requirement for more than one PTV may be that many PTVs do not carry a complete set of essential AZ molecules and that the incorporation of more than one PTV may be necessary for recruiting a complete set of these essential molecules (see Introduction).

To assess the variability in molecular content of individual PTVs, we labeled neurons with antibodies against Piccolo and Bassoon and compared the resulting immunofluorescence in individual PTVs. PTVs were distinguished from synapses by concomitant immunolabeling against Synapsin I as described above. As shown in Figure 8A, most Piccolo-positive, Synapsin I-negative puncta (presumably PTVs) were also positive for Bassoon (80%–85%, two experiments, n = 891). While most PTVs were observed to carry detectable amounts of both Piccolo and Bassoon, a quantitative comparison of the immunofluorescence of these two molecules on individual PTVs (Figure 8B) suggests that the relative content of these molecules on individual PTVs is variable (R = 0.48–0.56). Interestingly, in spite of the high degree of colocalization of these molecules at synapses (98%–99%, two experiments, n = 730; see also tom Dieck et al., 1998; Fenster et al., 2000), the immunofluorescence correlation at synaptic puncta was not much higher (R = 0.51–0.59). In comparison, a colocalization analysis using two different anti-Bassoon antibodies revealed a much higher degree of localization (96%–97%), and a stronger correlation between the labeling intensities of the two anti-Bassoon antibodies (R = 0.78–0.82, two experiments, n = 1020; Figure 8C). These data suggest that the limited colocalization and immunofluorescence intensity correlation observed for Bassoon and Piccolo at individual PTVs stems, at least in part, from some heterogeneity/variability in PTV molecular content.

To evaluate whether PTV molecular heterogeneity is unique to Piccolo and Bassoon or occurs for other AZ proteins, we assessed quantitative relationships with a third AZ protein, RIM, that was also found to be present on PTVs (Figures 1 and 2; see also Ohtsuka et al., 2002). This was accomplished by triple labeling neurons with antibodies against RIM, Bassoon, and Synapsin I (Figure 8D). As shown in Figure 8E, most of the Synapsin I-negative Bassoon puncta (presumably PTVs) were observed to colocalize with RIM (75%–82%, four experiments, n = 2225). In contrast, practically all synaptic (Synapsin I positive) Bassoon clusters were observed to colocalize with RIM (95%–99%, four experiments, n = 3260). A comparison of the immunofluorescence intensities of RIM and Bassoon on individual PTVs (Figure 8F) suggests that their quantitative relationships on individual PTVs are also variable (R = 0.55 ± 0.08, four experiments, n = 1801). Here too, as with Bassoon and Piccolo, the correlation of RIM and Bassoon at synaptic sites was not very different (0.60 ± 0.11, four experiments, n = 3015). Altogether, these experiments suggest that while most PTVs carry Bassoon, Piccolo, and RIM, the quantitative relationships of these molecules on individual PTVs are not fixed.

Synaptic RIM Can Be Accounted for by Unitary Insertion of PTVs

The findings and analyses described so far indicate that most nascent synapses may be formed by the recruitment of two to three PTVs. To further test this hypothesis, we performed two types of analyses to determine if a unitary analysis (such as that shown in Figure 6) performed for one PTV-associated AZ molecule (Bassoon) predicts correctly the synaptic content of another PTV-associated AZ molecule (RIM).

We first performed this analysis in "binary fashion" using the assumptions of binary distribution. Here we asked what would be the expected fraction of presynaptic sites in which RIM would be detected under the following assumptions: (1) RIM is detected on 75%–82% of PTVs (see previous section); (2) the fractions of presynaptic sites composed of one, two, three, four, or five PTVs are those calculated above for Bassoon (see Figure 6), and (3) PTVs are inserted randomly into nascent presynaptic sites. As shown in Figure 9A, the expected fraction of RIM-positive presynaptic sites was calculated to be 97%, which agrees well with the measured fraction of RIM-positive presynaptic sites (95%–99%).

We then performed a more quantitative analysis. Here we asked if the immunofluorescence intensity distribution of synaptic RIM could be predicted correctly from a unitary analysis performed for Bassoon in the same experiment. To this end, histograms of the immunofluorescence intensity of synaptic and PTV-associated RIM puncta were generated (Figure 9B). Then, a family of curves was calculated for the expected intensity distributions for multiples of PTV-associated RIM puncta, in a manner identical to that performed for Bassoon and Piccolo in Figures 6A–6C. In parallel, a similar analysis was performed for synaptic and nonsynaptic Bassoon, and the best fit in terms of the fraction of boutons composed of one to five PTVs was determined (Figure 9D). Finally, these fractions (calculated for *Bassoon*) were used as weights to generate predicted immunofluorescence distribution curves for synaptic *RIM* puncta after

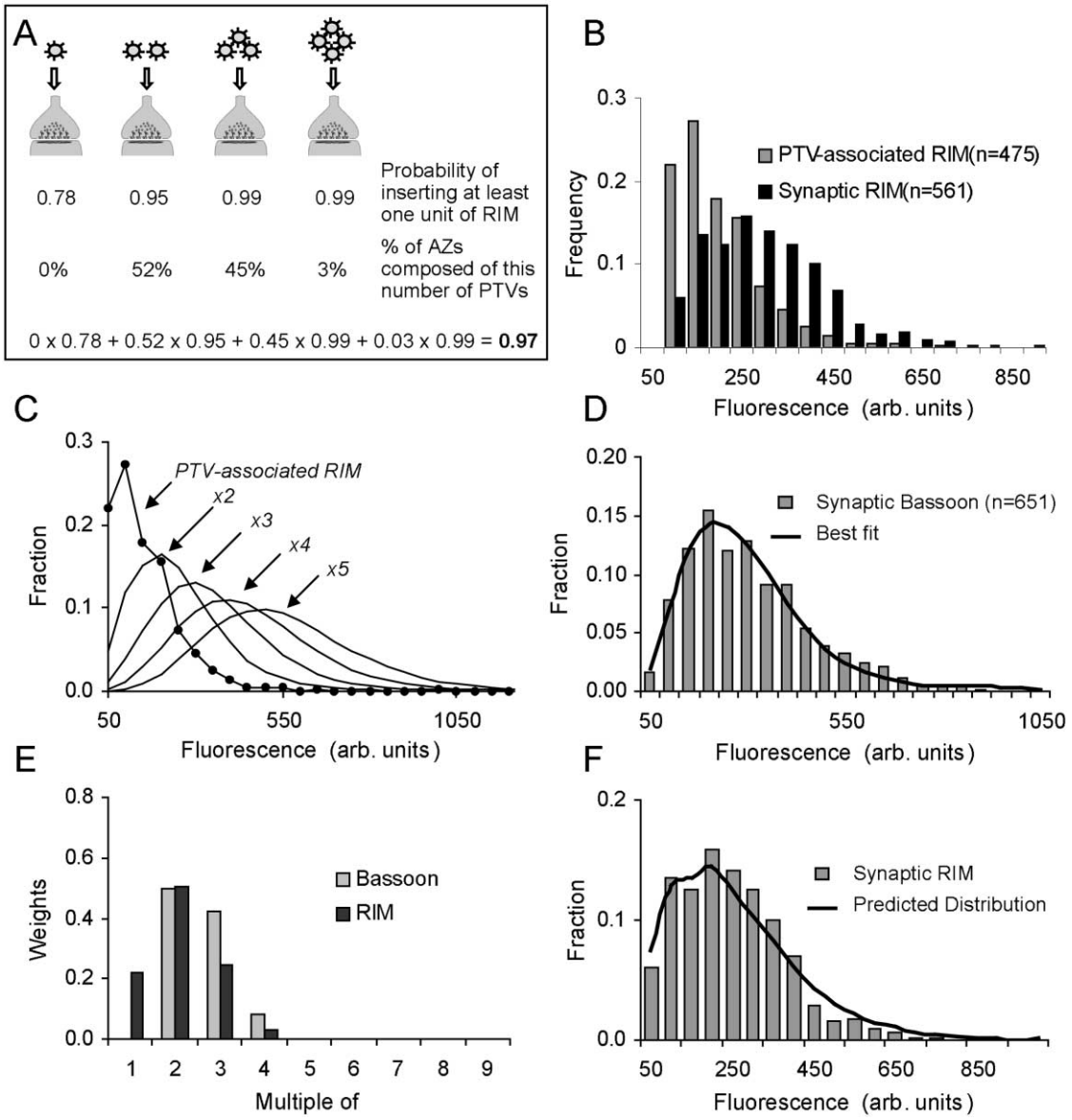

Figure 9. The Pool of Synaptic RIM Can Be Predicted from a Unitary Analysis for Bassoon

(A) An illustration of the calculation used to determine the expected fraction of presynaptic sites in which RIM should be detected, given that RIM is detected on 78% of PTVs. See text for details.

(B) Intensity histograms of PTV-associated RIM (Bassoon-positive, Synapsin I-negative RIM puncta) and of synaptic RIM (Bassoon- and Synapsin I-positive RIM puncta). All data obtained from one culture dish.

(C) Immunofluorescence intensity distribution of PTV-associated RIM clusters (filled circles) and calculated fluorescence intensity distributions for integer multiples of such puncta.

(D) In parallel, an analysis similar to that shown in Figure 6 was performed to determine the fraction of synapses composed of one, two, three, four, or five units of Bassoon. In this particular experiment, the best fit for Bassoon was obtained with the following values: two units, 50%; three units, 42%; four units, 8%.

(E) These weights were then used to calculate the fractions of synapses that would be expected to contain one to five units of RIM. This was necessary because not all nonsynaptic Bassoon puncta carried detectable amounts of RIM (see panel [A]). Assuming that PTV insertion was random and independent and given that 79% of the nonsynaptic Bassoon puncta were RIM positive in this experiment, the fractions of synapses expected to contain u units of RIM were $u = 0$, 3%; $u = 1$, 21%; $u = 2$, 49%; $u = 3$, 24%; $u = 4$, 3% (see Experimental Procedures).

(F) These fractions were then used as weights for calculating a weighted sum of the curves in panel (C), resulting in the predicted distribution of synaptic RIM immunofluorescence (black line). Note the good fit with the experimentally measured distribution of synaptic RIM immunofluorescence.

correcting for the experimentally determined fraction of RIM-positive Bassoon puncta (Figure 9E; see Experimental Procedures for details), and these curves were compared to the experimentally obtained distributions of synaptic RIM puncta immunofluorescence intensities (as exemplified in Figure 9F). In all four experiments, the

predicted curves agreed very well with the experimental data. Thus, a unitary analysis performed for one PTV molecule (Bassoon) predicts the synaptic distribution of a second PTV molecule (RIM) in the same experiment, strongly supporting the hypothesis that these molecules are recruited to synapses together and in unitary fashion.

Discussion

We have sought to examine the hypothesis that PTVs constitute a major form of AZ precursor vesicles and that AZs may be assembled from the unitary insertion of a small number of PTVs into the presynaptic membrane. This hypothesis is supported by several lines of experimental evidence. First, PTVs were found to carry many AZ proteins critically involved in the regulated exocytosis of SVs, including Bassoon, Piccolo, Syntaxin, RIM, Munc13, Munc18, SNAP25, Rab3a, and N-type calcium channels. Second, time-lapse imaging of GFP-tagged Bassoon revealed that PTVs are highly mobile, consistent with PTVs having a role in intracellular transport of AZ proteins to nascent synapses. Third, quantitative analysis indicates that PTVs carry a significant fraction of the Bassoon, Piccolo, and RIM content of individual synapses. Fourth, the synaptic content of Bassoon and Piccolo can be quantitatively described in terms of integer multiples of the PTV contents of these molecules. Finally, such integer multiples calculated for one PTV-associated AZ molecule (Bassoon) correctly predict the synaptic content of another AZ molecule (RIM). In addition, we find that the amounts of Bassoon, Piccolo, and RIM carried on individual PTVs exhibit some heterogeneity. Such variability in individual PTV content may make it necessary to insert more than one PTV into the presynaptic membrane in order to recruit a complete set of essential AZ molecules.

Are AZs Assembled from a Small Number of PTVs?

The conclusion that AZs may be assembled by the insertion of a small number (typically two to three) of PTVs into the presynaptic plasma membrane was based on the quantification and comparison of the Bassoon/Piccolo/RIM content of synaptic and nonsynaptic puncta of these molecules in cultured hippocampal neurons. In reaching this conclusion, several implicit assumptions were made that warrant some discussion.

The first assumption relates to the identity of nonsynaptic Bassoon/Piccolo/RIM puncta. Based on previous studies (Zhai et al., 2001), we assumed that nonsynaptic puncta observed in immunolabeled preparations represented individual PTVs. Yet, as the size of individual PTVs ($\sim$80 nm diameter) is much below the resolution of conventional light microscopy, the possibility that each of these puncta represents a cluster of PTVs cannot be ignored. One way to resolve this issue would be to examine the same nonsynaptic puncta at both light microscopy and EM levels. Yet, given the size of PTVs and the absence of additional structural markers (such as well formed PSDs), this type of analysis is not trivial to perform. It is worth noting that previously published EM micrographs suggest that PTVs travel along axons as individual vesicles (Zhai et al., 2001). It is likely, however, that some puncta within the nonsynaptic Bassoon and Piccolo populations were in fact pairs or triplets of PTVs. This would explain the rightward skewed distribution of intensity histograms generated for these populations and would be consistent with observations in which two GFP-Bsn609-3938 puncta appeared to merge into single brighter punctum and vice versa.

The second assumption we made was that each synaptic cluster represents a single structurally defined active zone. If, however, a significant number of synaptic Bassoon/Piccolo clusters were located at boutons with multiple AZs or at boutons too close to be separable by light microscopy, the number of PTVs required for the formation of individual AZs would be expected to be smaller than our estimates. While this could introduce some interpretation errors, we believe they are not significant. First, a significant number of overlapping fluorescent puncta were excluded from analysis (see Experimental Procedures). Second, EM analysis of synapses formed in primary cultures of hippocampal neurons similar to those used here suggests that only about 20%–30% of boutons contain more than one AZ (Schikorski and Stevens, 1997). Thus, even if some of our data were obtained from multiple AZs, this would not be expected to introduce major errors in our interpretation.

Our conclusion that AZs can form from the fusion of two to three PTVs is supported by EM analysis of hippocampal synapses described by Schikorski and Stevens (1997). Here the average area of AZs in rat hippocampal neurons grown in culture for 14 days was reported to be $0.027 \pm 0.019\ \mu m^2$ (and $0.039 \pm 0.022\ \mu m^2$ in the intact mouse hippocampus). In comparison, the calculated membrane area of a single PTV with a diameter of 80 nm is $0.020\ \mu m^2$. Thus the *mean* membrane area ratios of AZs and PTVs are 1.4:1 to 2:1 (compare with the mean synaptic/mean nonsynaptic fluorescence ratios determined here to be 1.9:1). Interestingly, the distribution profile of Bassoon and Piccolo content at synaptic puncta (Figure 5) is remarkably similar to the distribution profile of active zonal area in the intact hippocampus (Figure 4A in Schikorski and Stevens, 1997). Altogether, these data suggest that the areas of AZs and their Bassoon/Piccolo/RIM content are tightly related and are consistent with our hypothesis that AZs are formed from AZ material carried on a very small number of PTVs (two to three).

Does AZ Assembly Occur in Unitary/Quantal Fashion?

Electrophysiological and EM studies of synaptic junctions has led to the hypothesis that the fusion of single SVs with the plasma membrane at AZs delivers a unitary amount or *quanta* of neurotransmitter (the "quantal hypothesis"; Fatt and Katz, 1952; del Castillo and Katz, 1954). Traditionally, the quantal nature of a processes is examined by generating amplitude frequency histograms for the phenomena in question and scrutinizing them for discrete peaks at integer multiples of the amplitude of the single quantum. No unambiguous peaks were observed in our analysis, but given the variance in the fluorescence intensities measured for nonsynaptic Bassoon/Piccolo puncta, no such peaks were expected (see Figures 6A–6C). Some of this variance undoubtedly results from measurement noise and from the quantifi-

cation method used here (indirect immunofluorescence), yet it is more than likely that some of this variance is genuine (see below). Regardless of the reasons for the observed variance, the unit size of active zone material does not appear to be an entirely fixed value. Thus, strictly speaking, presynaptic assembly does not seem to be a classical "quantal" process. Yet, our unitary analysis is in full agreement with the possibility that synaptic AZs are formed by the insertion of integer numbers of the amounts of Bassoon (Figures 6 and 7) and Piccolo (Figure 6) carried on PTVs. Furthermore, the number of Bassoon units calculated to give the best fit for synaptic Bassoon predicted very well the expected intensity distribution of RIM at synapses (Figure 9). This result is fully consistent with the possibility that all three molecules are inserted together into the presynaptic membrane as a preformed unit. As PTVs are vesicles, they are excellent candidates for delivering such unitary amounts of AZ material to the plasma membrane. Thus, in spite of some variability in the molecular contents of individual PTVs, the insertion of PTVs with the plasma membrane is likely to deliver unitary amounts of AZ material to the nascent synapses. In this respect, AZ assembly might be loosely considered to be quantal in nature.

Are AZs Assembled from a Single Type of Precursor Vesicles?

Our biochemical and immunohistochemcal analysis of immunoisolated PTVs indicates that numerous components of the SV exocytosis machinery are present in these preparations. These included the α and β subunits of the N-type calcium channel, the t-SNAREs, Syntaxin and SNAP25, regulators of SV exocytosis, Rab3a, Munc13, Munc18, and RIM as well as structural proteins of the active zone, Piccolo and Bassoon. However, the amounts of Piccolo, Bassoon, and RIM on individual PTVs appeared to be somewhat variable (Figure 8). Undoubtedly, some of the observed variability stems from measurement noise and limitations inherent to indirect immunofluorescence, limitations that become evident when the labeling of the same molecule with two antibodies is compared (Figure 8C). Yet, similar comparisons performed for two different molecules revealed greater degrees of variability (Figures 8B and 8F), indicating that the quantitative relationships of AZ molecules on individual PTVs are not fixed.

The observed variability in PTV content may indicate that PTVs comprise a *family* of transport vesicle types, with each family having its own well-defined and highly regulated composition. In this situation, heterogeneity in AZ protein content would occur as a consequence of the subtype of PTVs inserted into the developing presynapse. While this possibility cannot be ruled out, we favor a more simple interpretation, wherein the biogenesis fidelity of PTVs is not high, and that the particular amounts of AZ molecules carried on individual PTVs are somewhat variable. Thus, several PTVs might be needed to recruit the full set of essential molecules required to transform a patch of presynaptic membrane into a functional AZ. The analysis we performed for RIM agrees well with this possibility, as it shows that even if only about 3/4 of PTVs carry RIM, insertion of two to three PTVs into presynaptic sites practically guarantees that most presynaptic sites will contain RIM (Figure 9A). It should be noted, however, that the situation becomes much more complicated when the recruitment of multiple presynaptic molecules is considered. Thus further work is necessary to determine if PTV content variability is a key factor in determining the number of PTVs recruited to the presynaptic membrane of nascent synapses.

At present, the functional consequences of PTV heterogeneity are not known. It is tempting to speculate, however, that PTV heterogeneity may underlie much of the heterogeneity displayed by individual synapses—even those originating from a single neuron—in terms of size, fine structure, molecular composition, and function (reviewed in Staple et al., 2000; Craig and Boudin, 2001; Atwood and Karunanithi, 2002). For example, even presynaptic boutons in autaptic cultures can be somewhat heterogeneous in their composition of Piccolo and Bassoon (Altrock et al., 2003) or Munc13-1 and Munc13-2 (Rosenmund et al., 2002). It remains to be seen, however, how much of this heterogeneity can be attributed to stochastic processes involved in PTV biogenesis and recruitment and how much results from more specific, tightly controlled processes (Craig and Boudin, 2001).

Experimental Procedures

Materials

The rabbit Bassoon antisera raised against a 75 kDa GST-Bassoon fusion protein and polyclonal rabbit Piccolo antibody against the GST-44a2 fusion protein were described previously (Cases-Langhoff et al., 1996; tom Dieck et al., 1998). Other antibodies used were as follows: mouse monoclonal anti-Synaptophysin, mouse monoclonal anti-SNAP25, mouse monoclonal anti-VAMP/Synaptobrevin II (Roche Diagnostics GmbH, Mannheim, Germany); mouse monoclonal anti-Rab3a, mouse monoclonal anti-RIM, mouse monoclonal anti-Munc18, mouse monoclonal anti-Munc 13-1 (Transduction Laboratories). Mouse monoclonal anti-α subunit of Calcium channels (a generous gift from Dr. Maureen McEnery, Case Western Reserve University School of Medicine), anti-β subunit of Calcium channel (Transduction Laboratories), mouse monoclonal anti-Synapsin I (Chemicon International Inc., CA), polyclonal guinea pig anti ProSAP1 (a generous gift of Dr. Tobias Böckers, University of Muenster, Germany), and Rabbit polyclonal anti-Syntaxin antibody (a generous gift of Dr. M. Quick, University of Alabama at Birmingham).

Light Brain Membrane Preparation, Immunoisolation, and Immuno-EM

E18 brains were dissected out and homogenized in homogenization buffer (5 mM HEPES [pH 7.4], 0.5 mM EDTA, 0.3 M sucrose, protease inhibitor cocktail). Homogenate was centrifuged at 800 $\times$ *g* for 20 min, and the crude membrane in the supernatant was hypotonically lysed by adding nine volumes of H_2O. The crude membrane was then centrifuged at 100,000 $\times$ *g* for 1 hr. The pellet (P100) and the supernatant (S100) fractions were adjusted to 2 M sucrose and loaded as a layer of a discontinuous sucrose gradient underneath layers of 1.2 M, 0.8 M, and 0.3 M sucrose. The sucrose gradient was centrifuged at 350,000 $\times$ *g* for 3 hr. Fractions were taken from the top of the gradient to the bottom. Immunoisolations were performed with tosylated superparamagnetic beads (Dynabeads M-500 Subcellular; Dynal Inc., NY) as described (Zhai et al., 2001).

For EM, light membrane fractions (0.3/0.8 M sucrose interface) were incubated with control IgG or Piccolo-rAb beads. After extensive wash, beads were incubated with monoclonal antibodies against Synaptophysin, Bassoon, RIM, or Munc18, followed by 5 nm gold-conjugated anti-mouse secondary antibody. The beads were then collected, extensively washed, fixed by 1% glutaldehyde, 4% paraformaldhyde, 1% tannic acid, and processed for EM.

Cell Culture and Transfection

Hippocampal cell cultures were prepared from CA1-CA3 regions of 1–2 day old Sprague-Dawley rats as described previously (Bresler et al., 2001). Experiments were performed on preparations grown in culture for 5–11 days.

Transfection of hippocampal neurons with GFP-Bsn609-3938 was based on the calcium phosphate transfection method described elsewhere (Bresler et al., 2001). Transfection was evaluated after 24–72 hr by fluorescence microscopy. Expression of exogenous DNA was typically detected in two to five neurons per coverslip.

Microscopy

Images were acquired using a custom built confocal laser scanning microscope using Zeiss 100× 1.2 NA or 40× 1.3 N.A. Fluar objectives. EGFP and FM 4-64 were excited at 488 nm, and emissions were read using 500–545 nm band-pass and >630 nm long-pass filters, respectively (Chroma, VT). Alexa 488 fluorescence was recorded at 488 nm excitation/500–545 nm emission. Tetramethylrhodamine fluorescence was recorded at 532 nm excitation/570–610 nm emission, and Cy-5 fluorescence was recorded at 633 nm excitation/650 nm emission. All data were collected at 640 × 480 resolution, 12 bits/pixel. Time-lapse recordings of GFP-Bsn609-3938 were performed at one focal plane at slow scan rates (20 μs/pixel) with the confocal aperture nearly fully open. For these experiments, coverslips with neurons were mounted in a chamber heated to 37°C (Bresler et al., 2001) and perfused with Tyrodes saline (119 mM NaCl, 2.5 mM KCl, 2 mM CaCl2, 2 mM MgCl2, 25 mM HEPES, 30 mM glucose, buffered to pH 7.4). Labeling of functional presynaptic boutons with FM 4-64 [*N*-(3-triethylammoniumpropyl)-4-(*p*-dibutylaminostyryl)pyridinium, dibromide, Molecular Probes, OR] was performed as described previously (Bresler et al., 2001).

Images of immunolabeled cells were collected by averaging three frames at ten sections spaced 0.5–0.7 mm apart with the confocal aperture nearly fully closed.

Quantitative Immunohistochemistry

Neurons were fixed with a fixative solution consisting of 4% formaldehyde and 120 mM sucrose in phosphate-buffered saline (PBS) for 20 min. Cells were permeabilized for 10 min in fixative solution to which 0.25% Triton X-100 was added. Cells were washed three times in PBS, incubated in 10% bovine serum albumin (BSA) for 1 hr at 37°C, and incubated overnight at 4°C with primary antibodies in PBS and 1% BSA. Cells were then rinsed three times for 10 min with PBS and incubated for 1 hr at room temperature with secondary antibodies in PBS and 1% BSA. The cells were rinsed again with PBS, mounted, and imaged.

Primary antibodies used here were listed above. Secondary antibodies used were Cy5 donkey anti-guinea pig (Chemicon International Inc., CA), tetramethylrhodamine goat anti-rabbit (Molecular probes), and Alexa 488 goat anti-mouse (Molecular probes). All secondary antibodies were tested thoroughly in control experiments for cross-species reactivity by omitting in each case one of the primary antibodies used later. In the experiments of Figures 8D and 8E, monoclonal anti Synapsin I antibodies were prelabeled with Alexafluor 647 using the Zenon labeling kit from Molecular Probes and added after the immunolabeling of RIM and Bassoon was completed.

Image Analysis

All data analysis was performed on maximal intensity projections of Z section image stacks using software written by one of us (N.E.Z.). Quantitative analysis of immunolabeled preparations was performed as follows. Identically sized analysis boxes (8 × 8 pixels, approximately 1 × 1 μm) were placed and centered programmatically over fluorescence peaks of immunolabeled Bassoon or Piccolo puncta. Then, all boxes within a radius of 1 μm from another box were removed programmatically to exclude overlapping clusters from analysis. The average intensity in each box was then determined. Puncta were categorized as synaptic or nonsynaptic according to colocalization with Synapsin I and ProSAP1 clusters as explained in Results. Clusters of Synapsin I or ProSAP1 were defined as distinct spots whose peak fluorescence levels were at least twice that of the background fluorescence in their immediate vicinity. Background fluorescence levels were determined for each image in eight to ten boxes placed over puncta-free neuronal processes, and their averaged values were subtracted from all fluorescence measurements.

The expected intensity distribution curves of multiples of nonsynaptic clusters (Figures 6, 7, and 9) were generated using a macro written in Visual Basic that did the following. On the basis of the fluorescence intensity distribution of the nonsynaptic puncta, the intensity of every combination of nonsynaptic clusters and the occurrence probability for this combination were calculated, and the probabilities of all resulting intensities were added up. This was performed separately for pairs, triples, and so on in each data set. Then, a weighted sum of these curves was determined using weights that provided the best fit for the experimentally measured distribution of synaptic puncta as shown in Figure 6.

In the case of RIM (Figure 9), the weights used to generate the predicted curve were based on the weights that gave the best fit for Bassoon as explained above. However, these could not be used directly for RIM because RIM was not found on all nonsynaptic Bassoon puncta. Thus, R_u, the fraction of synapses containing u unitary amounts of RIM (the weight assigned to the curve calculated for u multiples of RIM units) was determined for every u according to binomial distribution considerations and the following equation:

$$R_u = \sum_{n=1}^{5} f_n \binom{n}{u} p^u (1-p)^{n-u}$$

where f_n is the fraction of synapses determined to be assembled from n (going from 1 to 5) unitary amounts of Bassoon, and p is the fraction of nonsynaptic Bassoon puncta (presumably PTVs) positive for RIM.

Expression levels GFP-Bsn609-3938 were estimated as described previously for SAP90/PSD-95 (Bresler et al., 2001). Motion analysis of GFP-Bsn609-3938 clusters was performed by generating digital movies of time-lapse sequences and tracking the same clusters in consecutive frames. Analysis was performed backward in time from the moment of fixation, to facilitate identification of the same clusters in the immunolabeled tissue.

Quantitative analysis of GFP-Bsn609-3938 puncta intensity was done as described above for immunolabeled puncta except that here the analysis box size was 10 × 10 pixels (~1.5 μm × 1.5 μm). Final figures were prepared using commercial software (Adobe Photoshop, Microsoft Excel, and Microsoft PowerPoint).

Acknowledgments

We are grateful to Larisa Goldfeld, Vladimir Lyakhov, Ed Philips, and Jose Galaz for their invaluable technical assistance; to Tobias Böckers for providing ProSAP1 antibodies; Dr. Maureen McEnery for Calcium Channel antibodies; and to Drs. Stefan Kindler and Pedro Zamorano for their support and many stimulating discussions; and Dr. Johanna Montgomery for her critical eye in preparing this manuscript. This work was supported by grants from the National Institutes of Health (RO1 NS39471, PO1-HD38760, P50-HD32901) to C.C.G., the Deutsche Forschungsgemeinschaft (Gu230/4-1) and the Fonds der Chemischen Industrie to E.D.G, and the United States Israel Binational Science Foundation (2000232) and German Israel Foundation (686/2000) to N.E.Z.

Received: April 19, 2002
Revised: February 19, 2003
Accepted: March 10, 2003
Published: April 23, 2003

References

Ahmari, S.E., and Smith, S.J. (2002). Knowing a nascent synapse when you see it. Neuron *34*, 333–336.

Ahmari, S.E., Buchanan, J., and Smith, S.J. (2000). Assembly of presynaptic active zones from cytoplasmic transport packets. Nat. Neurosci. *3*, 445–451.

Altrock, W.D., tom Dieck, S., Sokolov, M., Meyer, A.C., Sigler, A., Brakebusch, C., Fassler, R., Richter, K., Boeckers, T.M., Potschka,

H., et al. (2003). Functional inactivation of a fraction of excitatory synapses in mice deficient for the active zone protein bassoon. Neuron *37*, 787–800.

Antonova, I., Arancio, O., Trillat, A.C., Wang, H.G., Zablow, L., Udo, H., Kandel, E.R., and Hawkins, R.D. (2001). Rapid increase in clusters of presynaptic proteins at onset of long-lasting potentiation. Science *294*, 1547–1550.

Atwood, H.L., and Karunanithi, S. (2002). Diversification of synaptic strength: presynaptic elements. Nat. Rev. Neurosci. *3*, 497–516.

Augustin, I., Rosenmund, C., Sudhof, T.C., and Brose, N. (1999). Munc13-1 is essential for fusion competence of glutamatergic synaptic vesicles. Nature *400*, 457–461.

Boeckers, T.M., Kreutz, M.R., Winter, C., Zuschratter, W., Smalla, K.-H., Sanmarti-Vila, L., Wex, H., Langnaese, K., Bockmann, J., Garner, C.C., and Gundelfinger, E.D. (1999). Proline-rich synapse-associated protein-1/cortactin binding protein 1 (ProSAP1/CortBP1) is a PDZ-domain protein highly enriched in the postsynaptic density. J. Neurosci. *19*, 6506–6518.

Bresler, T., Ramati, Y., Zamorano, P.L., Zhai, R., Garner, C.C., and Ziv, N.E. (2001). The dynamics of SAP90/PSD95 recruitment to new synaptic junctions. Mol. Cell. Neurosci. *18*, 149–167.

Brose, N., Rosenmund, C., and Rettig, J. (2000). Regulation of transmitter release by Unc-13 and its homologues. Curr. Opin. Neurobiol. *10*, 303–311.

Cases-Langhoff, C., Voss, B., Garner, A.M., Appeltauer, U., Takei, K., Kindler, S., Veh, R.W., De Camilli, P., Gundelfinger, E.D., and Garner, C.C. (1996). Piccolo, a novel 420 kDa protein associated with the presynaptic cytomatrix. Eur. J. Cell Biol. *69*, 214–223.

Colicos, M.A., Collins, B.E., Sailor, M.J., and Goda, Y. (2001). Remodeling of synaptic actin induced by photoconductive stimulation. Cell *107*, 605–616.

Craig, A.M., and Boudin, H. (2001). Molecular heterogeneity of central synapses: afferent and target regulation. Nat. Neurosci. *4*, 569–578.

Dai, Z., and Peng, H.B. (1996). Dynamics of synaptic vesicles in cultured spinal cord neurons in relationship to synaptogenesis. Mol. Cell. Neurosci. *7*, 443–452.

De Camilli, P., Harris, S.M., Jr., Huttner, W.B., and Greengard, P. (1983). Synapsin I (Protein I), a nerve terminal-specific phosphoprotein. II. Its specific association with synaptic vesicles demonstrated by immunocytochemistry in agarose-embedded synaptosomes. J. Cell. Biol. *96*, 1355–1373.

del Castillo, J., and Katz, B. (1954). Quantal components of the end-plate potential. J. Physiol. *124*, 560–573.

Dresbach, T., Qualmann, B., Kessels, M.M., Garner, C.C., and Gundelfinger, E.D. (2001). The presynaptic cytomatrix of brain synapses. Cell. Mol. Life Sci. *58*, 94–116.

Fatt, P., and Katz, B. (1952). Spontaneous sub-threshold activity at motor nerve endings. J. Physiol. *117*, 109–128.

Fenster, S.D., Chung, W.J., Zhai, R., Cases-Langhoff, C., Voss, B., Garner, A.M., Kaempf, U., Kindler, S., Gundelfinger, E.D., and Garner, C.C. (2000). Piccolo, a presynaptic zinc finger protein structurally related to bassoon. Neuron *25*, 203–214.

Garner, C.C., Zhai, R.G., Gundelfinger, E.D., and Ziv, N.E. (2002). Molecular mechanisms of CNS synaptogenesis. Trends Neurosci. *25*, 251–258.

Hopf, F.W., Waters, J., Mehta, S., and Smith, S.J. (2002). Stability and plasticity of developing synapses in hippocampal neuronal cultures. J. Neurosci. *22*, 775–781.

Ishizuka, T., Saisu, H., Odani, S., and Abe, T. (1995). Synaphin: a protein associated with the docking/fusion complex in presynaptic terminals. Biochem. Biophys. Res. Commun. *213*, 1107–1114.

Kraszewski, K., Mundigl, O., Daniell, L., Verderio, C., Matteoli, M., and De Camilli, P. (1995). Synaptic vesicle dynamics in living cultured hippocampal neurons visualized with CY3-conjugated antibodies directed against the lumenal domain of Synaptotagmin. J. Neurosci. *15*, 4328–4342.

Matteoli, M., Takei, K., Perin, M.S., Sudhof, T.C., and De Camilli, P. (1992). Exo-endocytotic recycling of synaptic vesicles in developing processes of cultured hippocampal neurons. J. Cell Biol. *117*, 849–861.

Nakata, T., Terada, S., and Hirokawa, N. (1998). Visualization of the dynamics of synaptic vesicle and plasma membrane proteins in living axons. J. Cell Biol. *140*, 659–674.

Ohtsuka, T., Takao-Rikitsu, E., Inoue, E., Inoue, M., Takeuchi, M., Matsubara, K., Deguchi-Tawarada, M., Satoh, K., Morimoto, K., Nakanishi, H., and Takai, Y. (2002). Cast: a novel protein of the cytomatrix at the active zone of synapses that forms a ternary complex with RIM1 and munc13-1. J. Cell Biol. *158*, 577–590.

Okabe, S., Miwa, A., and Okado, H. (2001). Spine formation and correlated assembly of presynaptic and postsynaptic molecules. J. Neurosci. *21*, 6105–6114.

Roos, J., and Kelly, R.B. (2000). Preassembly and transport of nerve terminals: a new concept of axonal transport. Nat. Neurosci. *3*, 415–417.

Rosenmund, C., Sigler, A., Augustin, I., Reim, K., Brose, N., and Rhee, J.S. (2002). Differential control of vesicle priming and short-term plasticity by Munc13 isoforms. Neuron *33*, 411–424.

Schikorski, T., and Stevens, C.F. (1997). Quantitative ultrastructural analysis of hippocampal excitatory synapses. J. Neurosci. *17*, 5858–5867.

Schoch, S., Castillo, P.E., Jo, T., Mukherjee, K., Geppert, M., Wang, Y., Schmitz, F., Malenka R.C., and Sudhof, T.C. (2002). RIM1alpha forms a protein scaffold for regulating neurotransmitter release at the active zone. Nature *415*, 321–326.

Staple, J.K., Morgenthaler, F., and Catsicas, S. (2000). Presynaptic heterogenity: Vive la difference. News Physiol. Sci. *15*, 45–49.

Sudhof, T.C. (2000). The synaptic vesicle cycle revisited. Neuron *28*, 317–320.

Takahashi, S., Yamamoto, H., Matsuda, Z., Ogawa, M., Yagyu, K., Taniguchi, T., Miyata, T., Kaba, H., Higuchi, T., Okutani, F., and Fujimoto, S. (1995). Identification of two highly homologous presynaptic proteins distinctly localized at the dendritic and somatic synapses. FEBS Lett. *368*, 455–460.

tom Dieck, S., Sanmarti-Vila, L., Langnaese, K., Richter, K., Kindler, S., Soyke, A., Wex, H., Smalla, K.H., Kampf, U., Franzer, J.T., et al. (1998). Bassoon, a novel zinc-finger CAG/glutamine-repeat protein selectively localized at the active zone of presynaptic nerve terminals. J. Cell Biol. *142*, 499–509.

Vardinon Friedman, H., Bresler, T., Garner, C.C., and Ziv, N.E. (2000). Assembly of new individual excitatory synapses: Time course and temporal order of synaptic molecule recruitment. Neuron *27*, 57–79.

Verhage, M., Maia, A.S., Plomp, J.J., Brussaard, A.B., Heeroma, J.H., Vermeer, H., Toonen, R.F., Hammer, R.E., van den Berg, T.K., Missler, M., et al. (2000). Synaptic assembly of the brain in the absence of neurotransmitter secretion. Science *287*, 864–869.

Zhai, R., Vardinon Friedman, H., Cases-Langhoff, C., Becker, B., Eckart, D., Gundelfinger, E.D., Ziv, N.E., and Garner, C.C. (2001). Assembling the presynaptic active zone: Characterization of an AZ precursor vesicle. Neuron *29*, 131–143.

Ziv, N.E., and Garner, C.C. (2001). Principles of glutamatergic synapse formation: seeing the forest for the trees. Curr. Opin. Neurobiol. *11*, 536–543.